部分電離プラズマにおけるケルビン・ヘルムホルツ不安定性の非線形の時間発展の研究
On the nonlinear evolution of the partially ionised Kelvin-Helmholtz instability

○ Andrew Hillier, 花山天文台, 〒607-8471 京都市山科区北花山大峰町, E-mail:andrew@kwasan.kyoto-u.ac.jp

玉澤 春史, 花山天文台, 〒607-8471 京都市山科区北花山大峰町, E-mail:tamazawa@kwasan.kyoto-u.ac.jp

中村 尚樹, 花山天文台, 〒607-8471 京都市山科区北花山大峰町, E-mail:nakamura@kwasan.kyoto-u.ac.jp

高棹 真介, 花山天文台, 〒607-8471 京都市山科区北花山大峰町, E-mail:takasao@kwasan.kyoto-u.ac.jp

Andrew Hillier, Kwasan Observatory, 17-1 Kitakazan-ohmine-cho, Yamashina-ku, Kyoto, 607-8471
Harafumi Tamazawa, Kwasan Observatory, 17-1 Kitakazan-ohmine-cho, Yamashina-ku, Kyoto, 607-8471
Naoki Nakamura, Kwasan Observatory, 17-1 Kitakazan-ohmine-cho, Yamashina-ku, Kyoto, 607-8471
Shinsuke Takasao, Kwasan Observatory, 17-1 Kitakazan-ohmine-cho, Yamashina-ku, Kyoto, 607-8471

The Kelvin-Helmholtz instability is found in many different situations in astrophysical systems. In the partially ionised plasma, plasma where the ionization fraction is less than unity, that are common throughout the universe this is no different. We investigate the linear and nonlinear dynamics of the Kelvin-Helmholtz instability in a partially ionised plasma using the new code under development by the MHD group of Kwasan Observatory, Kyoto University. Investigation of two cases, one where the coupling between the plasma and neutral fluid is weak, and another where the coupling is strong. The simulations show that the vortices created by the Kelvin-Helmholtz instability act as centrifuges that throw out the neutrals from the centre of the vortex, dynamically reducing the ionisation fraction in the vortex centre. This results may provide an observational test to show if the Kelvin-Helmholtz instability is occurring in physical systems where observations are not able to spatially resolve the vortex structure.

1. Introduction

In the swirling plasma found throughout the cosmos, the existence of shear flows is a natural state of affairs. When shear flows exist the Kelvin-Helmholtz instability, an instability that feeds off the kinetic energy of the shear flow to create vortices, is likely to form. The signature of this instability can be seen sometimes in clouds, in waves created by wind blowing across water and in Jupiter's red spot. In astrophysical systems, where magnetic fields are ubiquitous, the magnetic Kelvin-Helmholtz instability commonly occurs. For example in recent observations of the flanks of Coronal Mass Ejections in the solar corona (Foullon et al., 2011) and in-situ measurements of the Earth's magnetosphere (Hasegawa et al., 2004) the magnetic Kelvin-Helmholtz instability has been discovered.

For the simplest description of the magnetic Kelvin-Helmholtz instability in an incompressible plasma with discontinuous velocity shear, the condition for the onset of the instability is given by:

$$[k \cdot (V_1 - V_2)]^2 > \frac{\rho_1 + \rho_2}{4\pi \rho_1 \rho_2}[(k.B_1)^2 + (k.B_2^2)] \qquad (1)$$

Therefore, if the shear velocity is greater than the Alfven velocity of the plasma (using the component of the magnetic field parallel to the wavenumber), the system should be unstable to the growth of the Kelvin-Helmholtz instability. When the additional physics of ion-neutral coupling (relevent for plasma that is not fully ionised) is included, there are regimes in which sub-Alfvenic flows can excite the instability (Soler et al., 2012).

In many astrophysical cases, the temperatures are not sufficiently high to fully ionise the plasma. In molecular clouds, protoplanetary disks, cool stellar surfaces and even planetary atmospheres often very low ionisation fractions are found (i.e. $\xi_i \ll$ 10^{-3}). However, at the interface region between hot cornea and weakly ionised layers (where EUV irradiation from metal lines can become important), or the chromospheres of stars the ratio of ions to neutrals can approach , or even exceed, unity. This is the case even for plasmas of temperature $\leq 10^4$ K. In these cases, for example found in the chromosphere and in prominences of stars, the plasma is classified as partially ionised plasma. These interface layers are often found to be of great importance in terms of the energy transport and coupling between atmopsheric layers. It is in this regime that we investigate the dynamics of the magnetic Kelvin-Helmholtz instability.

2. Formulating the model for the partially ionised plasma simulations

2.1 The Partially Ionised Plasma Equations

For this study we follow the equations for a partially ionised plasma presented in Leake et al. (2012). First we detail the equations for the neutral fluid.

$$\frac{\partial \rho_n}{\partial t} + \nabla \cdot \rho_n v_n = 0 \qquad (2)$$

$$\frac{\partial \rho_n v_n}{\partial t} + \nabla \cdot [\rho_n v_n v_n + p_n I] = \qquad (3)$$
$$-\alpha_c \rho_p \rho_n (v_n - v_p)$$

$$\frac{\partial \varepsilon_n}{\partial t} + \nabla \cdot [(\varepsilon_n + P_n)v_n] = \qquad (4)$$
$$-v_n \cdot \alpha_c \rho_p \rho_n (v_n - v_p) + 0.5\alpha_c \rho_p \rho_n (v_n - v_p)^2$$
$$-3\alpha_c \rho_p \rho_n R_g (T_n - T_p)$$

where $\varepsilon_n = p_n/(\gamma - 1) + 0.5\rho_n v_n^2$. The subscripts n and p refer to the neutral fluid and the magnetised plasma

The equations for the magnetised plasma

$$\frac{\partial \rho_p}{\partial t} + \nabla \cdot \rho_p v_p = 0 \quad (5)$$

$$\frac{\partial \rho_p v_p}{\partial t} + \nabla \cdot \left[\rho_p v_p v_p + \left(p_p + \frac{B^2}{8\pi} \right) I - \frac{BB}{4\pi} \right] = \quad (6)$$

$$\alpha_c \rho_p \rho_n (v_n - v_p)$$

$$\frac{\partial B}{\partial t} = \nabla \times (v_p \times B) \quad (7)$$

$$\frac{\partial}{\partial t} \left(\varepsilon_p + \frac{B^2}{8\pi} \right) + \nabla \cdot \left[(\varepsilon_p + P_p) v_p + \frac{c}{4\pi} E \times B \right] = \quad (8)$$

$$v_p \cdot \alpha_c \rho_p \rho_n (v_n - v_p) + 0.5 \alpha_c \rho_p \rho_n (v_n - v_p)^2$$
$$+ 3 \alpha_c \rho_p \rho_n R_g (T_n - T_p)$$

where $\varepsilon_p = p_p / (\gamma - 1) + 0.5 \rho_p v_p^2$. In these equations, the collisional frequency ν_{pn} is given as $\alpha_c \rho_p$. In this initial study, the terms involving the ionisation and recombination of the plasma have been neglected.

2.2 The Scheme

In this study we use a fourth-order central difference scheme that uses a four-step Runge-Krutta scheme for the time advancement (Vögler et al., 2005). The artificial viscosity is based on the scheme presented in Rempel et al. (2009). This scheme forms part of the basis for a new partially ionised plasma scheme under development by the staff and students of Kwasan Observatory, Kyoto University.

In the temporal update of the scheme, the collision terms are solved separately from the dynamical terms. For simulations where the collision timescale is comparable to dynamic timescale, the collision terms are updated using a first-order integration. When the collision terms require a timestep that is less than 10% of the timestep required by the dynamic CFL condition, the collision terms are analytically integrated to give exponential solutions which are used to advance the scheme under significantly reduced constraints for the time advancement.

2.3 The Initial and Boundary Conditions

The domain is divided into two layers, upper and lower. The upper layer has a total density $\rho_U = 2$, and a velocity $V_{xU} = 1$. The lower layer has a total density $\rho_L = 2$, and a velocity $V_{xL} = -1$. The total pressure and magnetic field are initially uniform throughout the calculation domain with $P = 2.5$ and $B_z = 4 \times \sqrt{4\pi}$. For this study we take the neutral fraction to be $\xi_n = 0.5$ and $\gamma = 1.4$.

We use a grid of 200x200 with a grid size of $dx = 0.005$ and $dy = 0.01$. The boundary in the x-direction is taken to be periodic and the boundary in the y-direction is symmetric.

3. Results for the linear growth and nonlinear dynamics

Here we investigate development of the instability and then the nonlinear evolution for the configuration described above. The simulations are performed for two different values of α_c so that the changes in the dynamics between the weak and strong coupling regimes can be elucidated, as well as the different between the partially ionised regime and the ideal MHD regime.

3.1 Linear Regime

Panels a and b of Figure 1 shows the linear growth of the kinetic energy of the y velocity and its following nonlinear saturation for the case where $\alpha_c = 1$ and $\alpha_c = 100$ respectively. The clear difference between the two cases is that for $\alpha_c = 100$ the instability grows at the same rate and at the same level in both fluids, i.e.

the instability grows simultaneously in both fluids implying strong coupling between the fluids, but for the case where $\alpha_c = 1$ the instabilities grow at the same rate, but there is a delay between the magnitude of the instability between the fluids.
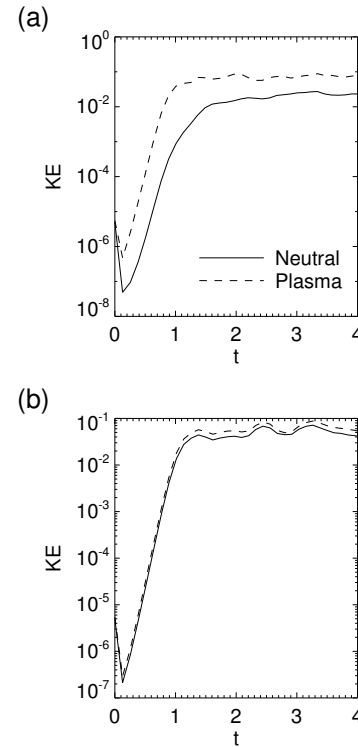

Fig. 1 The panels show the growth of the kinetic energy of the y velocity ($0.5\rho v_y^2$) at $x = 0$ for the plasma (dashed line) and the neutral fluid (solid line) for $\alpha_c = 1$ (panel a) and $\alpha_c = 100$ (panel b). The evolution is only shown up to $t = 4$.

It is the weak coupling case that is of more interest. Here the growth rate for both the fluids is the same, but the instability does not grow simultaneously. In this case the instability grows quickest in the ionised plasma, as this instability grows the coupling between the two fluids takes effect and the velocity difference between the ionised plasma and the neutral fluid becomes sufficiently large to have an effect through coupling terms. The instability is then excited in the neutral fluid through this coupling, growing with the same growth rate as the ionised plasma. Once the instability has saturated in the ionised plasma, the growthrate for the neutral plasma drops as there is no longer the continued growth of the instability in the plasma to drive it on, meaning it reverts back to its own smaller growth rate.

3.2 Nonlinear Dynamics

Figures 2 and 3 show the neutral and plasma densities for the the nonlinear evolution of the instability for both the the case where $\alpha_c = 1$ and $\alpha_c = 100$. Structurally, the main difference between the low α_c case and the high α_c case is the vortex shape in the neutral fluid. In the high α_c case, the vortices that form in the neutral fluid and ionised plasma are structurally very similar. However, for the low α_c case the neutral vortices are more elliptical, having a thin axis in the y direction and are more aligned with the flow. This will be a direct result of the greater compressible effects that

the neutral fluid is subject too as a result of the fast flow. As the ionised plasma is low β, and the sound speed in the plasma is faster than that of the fluid, it is only natural that in this large shear flow regime, the compressible effects will be significantly more noticeable in neutral fluid. For both cases the neutral fluid appears to contain sharper structure than the ionised plasma, which is more diffuse.

Panels c and f of both Figure 2 and Figure 3 show the ratio of neutrals to ions (ρ_n/ρ_p) throughout the calculation domain. The first point of note in this figure is that the centre of the vortices appear darker than the surrounding medium. This implies that there has been an increase in the ionization fraction in the centre of each vortex.

The arrows on these plots show the drift velocity ($V_n - V_p$). For Figure 2 the arrows have been drawn 2.5 times longer than those in the panels above and for Figure 3 the arrows have been made 5 times longer. This was done to make the direction of the drift velocity easier to see. These plots show that where the main flow velocity turns from the x-direction to the y-direction the drift velocity is largest. At these points, relatively speaking, the neutrals are flowing outward and the ions are flowing inward. From this we can learn that the vortices are acting like centrifuges, where the neutrals and ions are separated. The neutrals are thrown out of the vortex structure whilst the ions collect in the centre.

4. Vortices as centrifuges to separate the neutral fluid from the plasma

We have presented results for the development of the Kelvin-Helmholtz instability in a partially ionised plasma. The results can be summarised as follows:

1. Though the growth rate for the instability is the same in both fluids for both values of α_c. There is a delay for the instability in the low α_c case, showing that the instability is driven in the neutral fluid by the fluid being pulled along by the magnetized plasma, once the instability has grow sufficiently in the plasma itself.

2. The vortices created by the instability act like a centrifuge, throwing out the neutral fluid and collecting the ionised plasma in the centre.

3. In the weak coupling case the vortices in the neutral fluid are squashed in the y direction as a result of the high shearflow velocity leading to strong compressible effects.

The parameter regime that we have presented in this paper (especially that for the high α_c case) is one that can be expect to exist in astrophysical plasma. Observationally, if this was observed then the centre of the vortex should become dimmer when observed in lines from neutral atoms, and be enhanced in the lines from ionised plasma. This could be seen as one way of investigating if the K-H instability is occurring on scales where the observation of the fine vortex structure is difficult. Observations using the Solar Optical Telescope on the Hinode satellite of solar prominences and the solar chromosphere are potentially well suited for such a study.

参考文献

Foullon, C., Verwichte, E., Nakariakov, V. M., Nykyri, K., & Farrugia, C. J. 2011, The Astrophysical Journal Letters, 729, L

Hasegawa, H., Fujimoto, M., Phan, T.-D., et al. 2004, Nature, 430, 755

Leake, J. E., Lukin, V. S., Linton, M. G., & Meier, E. T. 2012, The Astrophysical Journal, 760, 109

Rempel, M., Schüssler, M., & Knölker, M. 2009, The Astrophysical Journal, 691, 64

Soler, R., Díaz, A. J., Ballester, J. L., & Goossens, M. 2012, The Astrophysical Journal, 749, 163

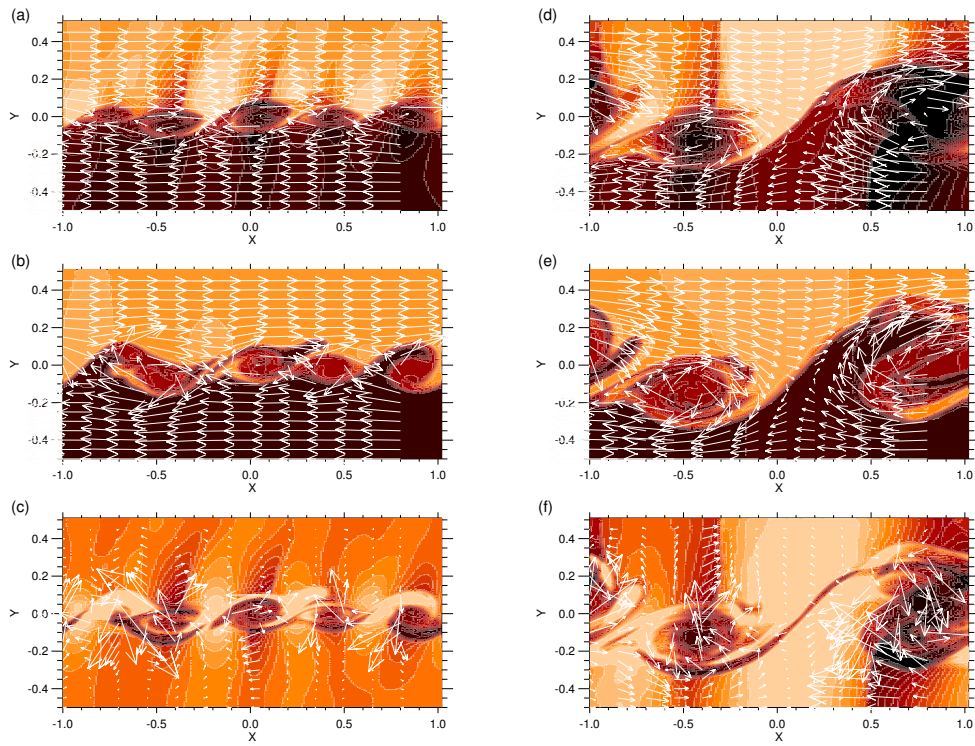Vögler, A., Shelyag, S., Schüssler, M., et al. 2005, Astronomy and Astrophysics, 429, 335

Fig. 2   The panels show the neutral density (top row), plasma density (middle row) and the ratio of neutrals to ions ρ_n/ρ_p (bottom row)for $t = 1.85$ (left column) and $t = 3.6$ (right column). The arrows show the neutral (top), plasma (middle) and drift $v_n - v_p$ (bottom) velocities.
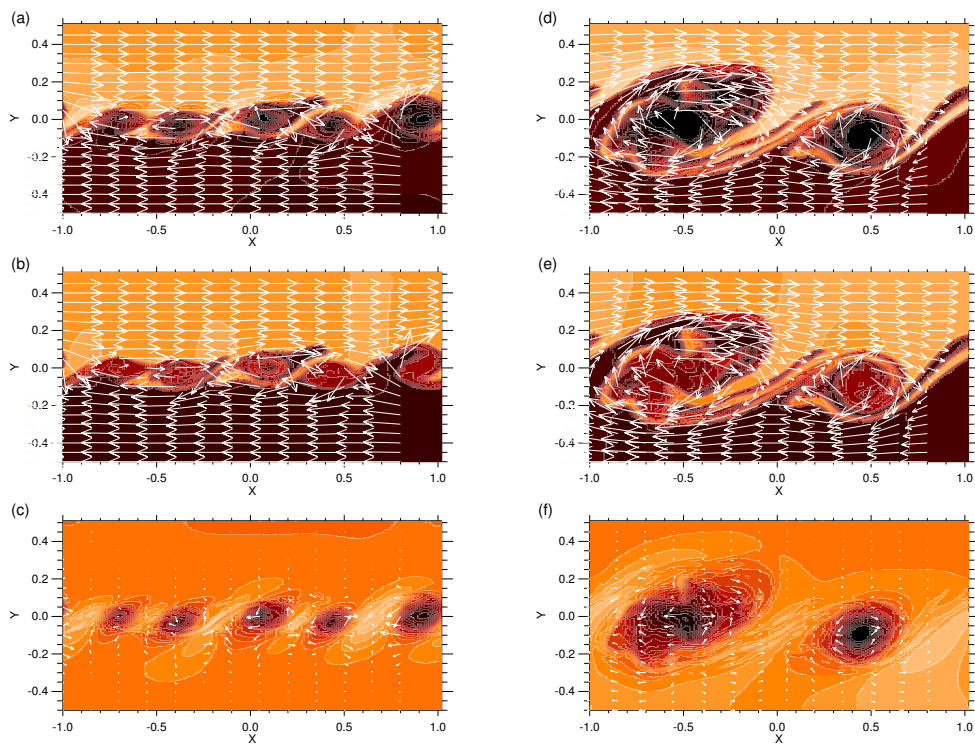

Fig. 3   The panels show the neutral density (top row), plasma density (middle row) and the ratio of neutrals to ions ρ_n/ρ_p (bottom row)for $t = 1.85$ (left column) and $t = 3.6$ (right column). The arrows show the neutral (top), plasma (middle) and drift $v_n - v_p$ (bottom) velocities.